A Reconfigurable In-band Digital Predistortion Technique for mmWave Power Amplifiers Excited by a Signal with 640 MHz Modulation Bandwidth

Chao Yu, Debin Hou, Honglei Sun, Fan Meng, Xiao-Wei Zhu, Jianfeng Zhai, Jixin Chen, Pinpin Yan
State Key Laboratory of Millimeter Waves,
Southeast University
Nanjing, China
chao.yu@seu.edu.cn

Anding Zhu
RF & Microwave Research Group
University College Dublin
Dublin, Ireland

***Abstract*—In this paper, a novel in-band digital predistortion (I-DPD) technique with a reconfigurable coefficient pyramid is proposed to linearize a mmWave power amplifier excited by a modulated signal with very large bandwidth, such as 640 MHz. This method can overcome the multiple bandwidth regrowth issue in conventional DPD operation that normally places a burden on the 5G applications. By employing a coefficient pyramid, the proposed method can efficiently select the necessary core functions to build the nonlinear kernels according to the operation modes, which can largely reduce the power consumption and thus increase the system efficiency. Experimental results with 640MHz modulated signal proves that extending the DPD capability into the forthcoming 5G is possible.**

Keywords—Digital predistortion; 5G mobile communication; mmWave; wideband; power amplifiers

I. INTRODUCTION

Large modulated bandwidth, such as more than 500 MHz, has been largely expected in the fifth-generation (5G) mobile communication deployment. It can provide very high data rate at the level of Gbps, satisfying the surging demand for data service, such as 8K TV broadcasting. Like the previous development in 3G/4G systems, the power amplifier (PA) in 5G will also suffer from power efficiency issue. To resolve the problem, the PA is required to be operated in the saturation region and thus inevitably introduces the nonlinear distortion into the system that can largely distort the in-band signal and generate the spectrum regrowth to affect the adjacent channel. This situation becomes severer when the larger modulation bandwidth transmission is adopted in the forthcoming 5G communication system.

To resolve this issue, proper linearization techniques must be employed to suppress the nonlinear distortion. Due to the merits of low cost, easy implementation and high accuracy, digital predistortion (DPD) [1] has become one of the most popular methods in PA linearization in the existing base stations. However, due to the large modulation bandwidth in 5G, the conventional DPD technique will face two main challenges: (i) the required digital signal processing data rate is too high for the existing digital chips; (ii) The analog bandwidth for both transmitter and feedback loop is also too wide which is not feasible to implement. These two challenges will place a huge burden on the application of DPD technique in the new scenarios in 5G.

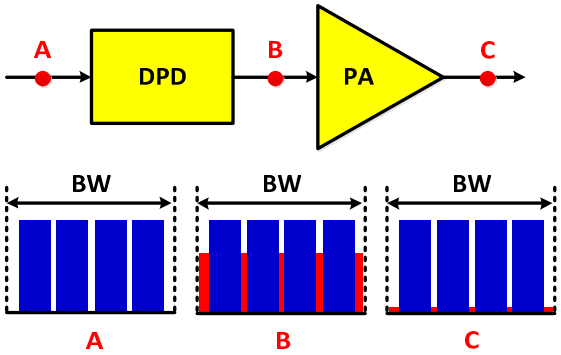

Fig.1. In-band digital predistortion concept.

Therefore, many studies have moved back to the analog predistortion technique that has the merit of large linearization bandwidth. However, the analog predistortion has intrinsic limitations on the linearization accuracy, which makes it difficult to deal with future high-order modulation transmission scheme, such as 4096 QAM.

In this paper, a novel in-band digital predistortion (I-DPD) technique is proposed to alleviate the challenges that the digital predistortion techniques are facing. In the meantime, the reconfigurability of the proposed I-DPD technique can enable flexibly changing the core functions according to the system operation mode, which will further enhance the DPD capability in the 5G era.

II. PROPOSED TECHNIQUE

The concept of I-DPD technique is illustrated in Fig. 1. Signal processing bandwidth is strictly limited to a specified bandwidth (BW), which means there is no extra spectrum regrowth required in the predistorted signal generation. By employing the I-DPD concept, the PA is required to design only for the specified bandwidth, which will be similar as the original input bandwidth. Thus, the out-of-band distortion can be removed by the designed PA itself, similar to the band-limited solution in [2].

A. In-band Distortion Decomposition

Since we have the limitation for the DPD processing bandwidth, all the nonlinear terms should be generated within the bandwidth without aliasing, and only the in-band distortion is our concern. To resolve this issue, the in-band distortion should be decomposed into smaller pieces to be generated within the specified bandwidth. To achieve this goal, the proposed idea is to channelize the input signal first into several signals with smaller bandwidth. Here, the in-band distortion can be divided into several distortion groups located at different channel, as shown in Fig. 2. The four channels are denoted as 1, 2, 3, 4, respectively. Ch 1: located at the center frequency for the first left band f_{-1} ; Ch 2: located at the center frequency for the first right band f_1; Ch 3: located at the center frequency for the second left band f_{-3}; Ch 4: located at the center frequency for the second right band f_3. Like the sideband compensation in [3], each distortion can be built by the core functions and the weighting envelope. Here, we further enhance the technique for the in-band kernel generation. The core functions are built by the 3rd-order intermodulation products (IM3), which is crucial for the nonlinear kernels generation. Different groups of core functions will be processed by different procedures. For example, in Fig.2, the core functions located at f_{-1} and f_1 will require the frequency shifting after the generation operations in the baseband, while the ones at f_{-3} and f_3 will require an extra filtering operation in the baseband before employing the frequency shifting.

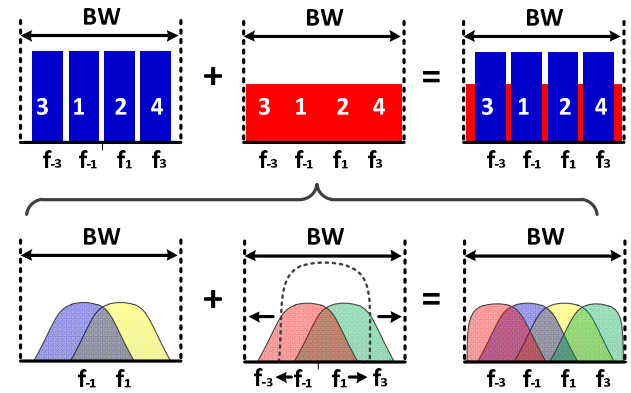

Fig.2. In-band distortion decomposition.

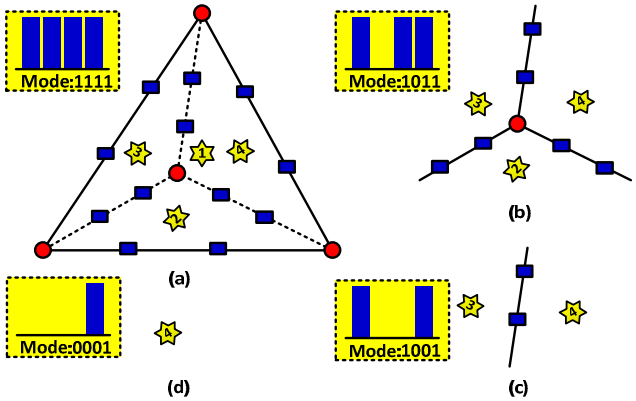

Fig.3. Reconfigurable coefficient pyramid for I-DPD . (a) 1111 model (2) 1011 model (3) 1001 model (4) 0001 mode

B. Reconfigurable Coefficient Pyramid

There is a great advantage for the in-band distortion decomposition. That is, only the necessary coefficient sets need to be selected according to the transmitted signal, while the unused ones can be switched off, which can effectively save the power consumption and thus increase the system efficiency. For example, as shown in Fig. 2, there are four carriers to form the transmitting signal by the carrier aggregation technique. However, in some moments, due to the few user resources, not all the carrier are required to be used for transmission and some of the carriers will be shut down. Here, for simplicity, we only list four common modes: 1111 (carrier 1, 2, 3, 4 on), 1011 (carrier 2, 3 ,4 on), 1001 (carrier 3 ,4 on), and 0001 (only carrier 4 on).

To efficiently obtain the core functions for different signal modes, we propose a reconfigurable coefficient pyramid structure for four carrier signals to switch on the necessary core functions, as shown in Fig. 3. In Fig. 3, the core functions in each model can be demonstrated by the corresponding mode pattern.

In this pyramid, the four facets represent the four carriers. The star symbol in yellow represents core functions generated by the facet itself (e.g. $\tilde{x}_{-1}\tilde{x}_{-1}\tilde{x}^*_{-1}$), the square symbol in blue on line represents the core functions generated by the neighbor facets (e.g.$\tilde{x}_{-1}\tilde{x}_1\tilde{x}^*_{-1}$), and the circle symbol in red represents the core function generated by all three neighbor facets (e.g. $\tilde{x}_1\tilde{x}_{-1}\tilde{x}^*_3$). As for the reconfigurable functions, if the signal model changes, the core function can be easily obtained by removing the related facets. Therefore, the full coefficient pyramid in Fig, 3a can be degenerated into the ones shown in Fig. 3b-3d, depending on the transmitted carriers. Therefore, this method can largely reduce the model complexity in the core function generation.

C. Model Structure

By employing the proposed technique discussed above, the I-DPD model can be built. Here, we take mode 1111 for example. Firstly, the original signal will be channelized into four signals based on the intrinsic nature of the carrier aggregation technique $\tilde{x}_{-1}, \tilde{x}_{1}, \tilde{x}_{-3}, \tilde{x}_{3}$.

The second step is to generate the core functions correctly. As shown in Fig.2, there should be four sets of core functions. In each set, the core functions, e.g. $\tilde{x}_a(n)\tilde{x}_b(n)\tilde{x}_c^*(n)$ can be found by the proposed reconfigurable coefficient pyramid.

Here, the model 1111 is taken for example. The core functions located at f_1,

$$\begin{cases} \tilde{x}^1_{C(1)} = \tilde{x}_{-1}(n)\tilde{x}_{-1}(n)\tilde{x}^*_{-3}(n) \\ \tilde{x}^2_{C(1)} = \tilde{x}_{-3}(n)\tilde{x}_{1}(n)\tilde{x}^*_{-3}(n) \\ \tilde{x}^3_{C(1)} = \tilde{x}_{-3}(n)\tilde{x}_{3}(n)\tilde{x}^*_{-1}(n) \\ \tilde{x}^4_{C(1)} = \tilde{x}_{-1}(n)\tilde{x}_{1}(n)\tilde{x}^*_{-1}(n) \\ \tilde{x}^5_{C(1)} = \tilde{x}_{1}(n)\tilde{x}_{1}(n)\tilde{x}^*_{1}(n) \\ \tilde{x}^6_{C(1)} = \tilde{x}_{-1}(n)\tilde{x}_{3}(n)\tilde{x}^*_{1}(n) \\ \tilde{x}^7_{C(1)} = \tilde{x}_{1}(n)\tilde{x}_{3}(n)\tilde{x}^*_{3}(n) \end{cases} \quad (1)$$

For the core functions located at f_3, they are only part of IM3 is required for modeling, as shown in Fig. 2. To correctly generate the core functions, the filter function $w(n)$ can be designed within a specified frequency range, which will be employed to remove the spectrum out of the edge, that is

$$\begin{cases} \tilde{x}^1_{C(3)} = \tilde{x}_{-3}(n)\tilde{x}_{3}(n)\tilde{x}^*_{-3}(n) * w_3(n) \\ \tilde{x}^2_{C(3)} = \tilde{x}_{-1}(n)\tilde{x}_{1}(n)\tilde{x}^*_{-3}(n) * w_3(n) \\ \tilde{x}^3_{C(3)} = \tilde{x}_{1}(n)\tilde{x}_{1}(n)\tilde{x}^*_{-1}(n) * w_3(n) \\ \tilde{x}^4_{C(3)} = \tilde{x}_{-1}(n)\tilde{x}_{3}(n)\tilde{x}^*_{-1}(n) * w_3(n) \\ \tilde{x}^5_{C(3)} = \tilde{x}_{1}(n)\tilde{x}_{3}(n)\tilde{x}^*_{1}(n) * w_3(n) \\ \tilde{x}^6_{C(3)} = \tilde{x}_{3}(n)\tilde{x}_{3}(n)\tilde{x}^*_{3}(n) * w_3(n) \end{cases} \quad (2)$$

After this operation, the correspondent core functions should be shifted into the right central frequencies to form the distortion in the predistorted signal. The core functions centered at $f_{-1}$and f_{-3}can also be generated by the same way.

The third step is to generate the average envelope to weigh the core functions in order to generate high order nonlinear kernels.

Therefore, the total model can build as

$$\tilde{y}(n) = \sum_{i=\{-3,-1,1,3\}} \sum_{m=0}^{M} h_{i,m}\tilde{x}_i(n-m)\, exp^{\frac{j2\pi f_i(n-m)}{f_s}}$$

$$+ \sum_{i=\{-1,1\}} \sum_{p=0}^{P} \sum_{m=0}^{M} \sum_{k=1}^{K1} h_{i,m,k}\tilde{x}^k_{C(i)}(n-m)\, exp^{\frac{j2\pi f_i(n-m)}{f_s}} e^p(n-m)$$

$$+ \sum_{i=\{-3,3\}} \sum_{p=0}^{P} \sum_{m=0}^{M} \sum_{k=1}^{K2} h_{i,m,k}\tilde{x}^k_{C(i)}(n-m)\, exp^{\frac{j2\pi f_i(n-m)}{f_s}}$$

$$* w_i(n-m)e^p(n-m)$$

Where P represents the order for the envelope, M is the memory length, K_1 and K_2 is the number of the core functions located at each carrier, and the weighting function generated by the average envelope $e(n)$ can be represented by

$$e(n) = \sqrt{|\tilde{x}_{-3}(n)|^2 + |\tilde{x}_{-1}(n)|^2 + |\tilde{x}_{1}(n)|^2 + |\tilde{x}_{3}(n)|^2} \quad (4)$$

III. Experimental Results

To effectively validate this concept, a wideband DPD test bench for 5G application was setup as shown in Fig, 4a. Firstly, the vector signal generator (Keysight M8190A) will generate a 640 MHz baseband signal withPAPR of 7.5 dB and then send the signal by Keysight E8267D to excite a mmWave GaAs PA with the average output power of 24 dBm and the center frequency of 29 GHz, whose chip layout is shown in Fig.4b. The P1dB for the PA output is 30.4 dBm. Then, the distorted output of the PA will pass through a 24 dB attenuator and be captured by the spectrum analyzer (Keysight N9040B). Both the input and output signal will be sent back to a PC and processed in the software Matlab for DPD model extraction and generation. In the model, the parameter M and P is set to 1. The data rate for all signal processing is limited to 1105.92 MSPS.

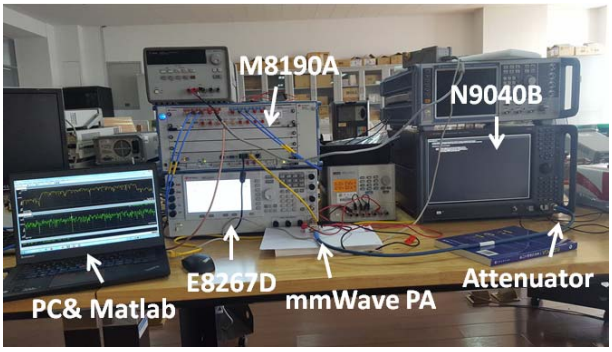

(a)

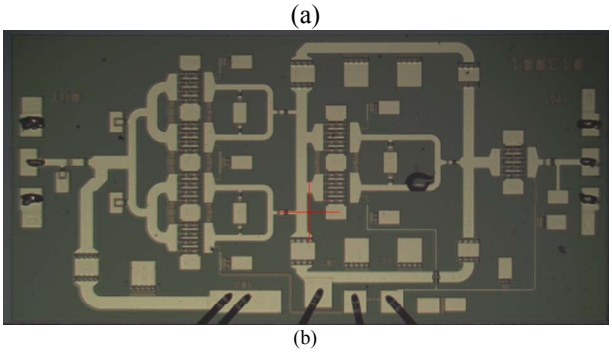

(b)

Fig.4. Measurement setup (a) test bench (b) PA chip layout

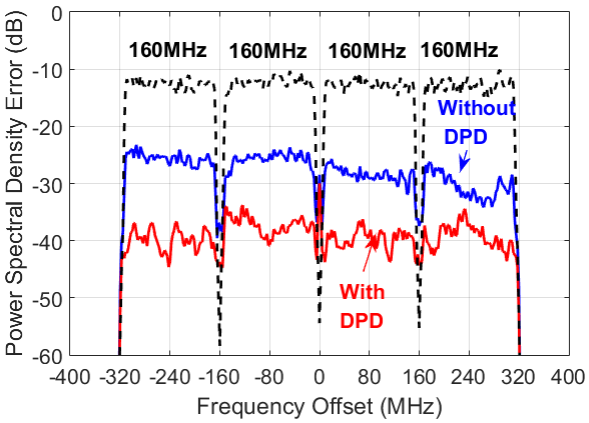

Fig. 5. Measured power spectrum errorfor 640 MHz signal

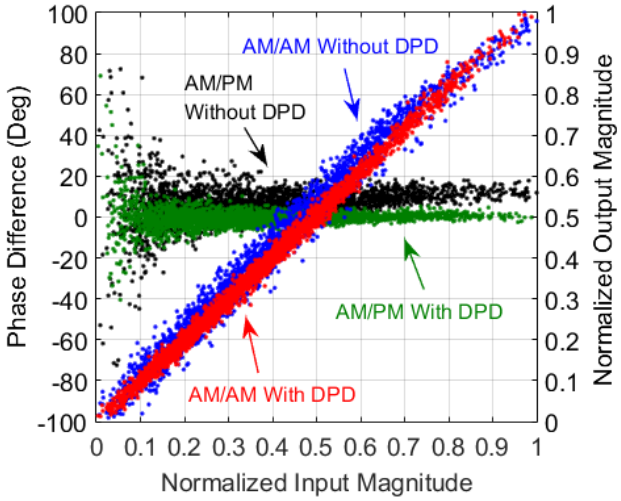

Fig. 6. Measured AM/AM,AM/PM curve for 640 MHz signal (a)AM/AM,AM/PM curve (b) power spectrum error

Fig. 5 shows the measured power spectrum error for 640 MHz signal. From Fig. 5, the proposed model will effectively reduce the in-band distortion by around 10 dB. It is worth mentioning that the out-of-band distortion has been filtered out in digital domain to correctly illustrate the in-band performance, which could be further removed by the previous work in [3]. Fig. 6 shows the AM/AM and AM/PM characteristics without/with DPD, which provides a linearization validation in time domain. It can be seen that the nonlinearity has been almost removed, but the performance is still not ideal compared to the conventional DPD performance. It should be noted that the noise floor for 640 MHz signal in the measurement setup is relatively high, which limits the linearization performance. The details for measurement performance have been listed in Table I.

TABLEI
THE MEASURED PERFORMANCE

Scenario	NRMSE
Without DPD	17.62%
With DPD	5.10%

IV. CONCLUSION

In this paper, a novel in-band DPD technique with a reconfigurable coefficient pyramid was proposed with the reconfigurabilities for different signal modes. The validation on 4-carrier 640 MHz bandwidth signal provides valuable potential to extend the DPD technique into future 5G applications.

ACKNOWLEDGMENT

This work is supported by the National Natural Science Foundation of China (NSFC) under Grant 61601117, 61401088, the Natural Science Foundation of Jiangsu Province under Grant BK20160698. The authors would like to thank Keysight technologies for providing the technical support in the measurement setup.

REFERENCES

[1] F. M. Ghannouchi and O. Hammi, "Behavioral modeling and predistortion," in *IEEE Microwave Magazine*, vol. 10, no. 7, pp. 52-64, Dec. 2009.

[2] C. Yu, L. Guan, E. Zhu, and A. Zhu, "Band-limited Volterra seriesbased digital predistortion for wideband RF power amplifiers," *IEEE Trans. Microw. Theory Techn.*, vol. 60, no. 12, pp. 4198–4208, Dec. 2012.

[3] C. Yu, H. Sun, X.-W. Zhu, W. Hong and A. Zhu, "A channelized sideband distortion model for suppressing unwanted emission of Q-band millimeter wave transmitters," *2016 IEEE MTT-S International Microwave Symposium (IMS)*, San Francisco, CA, 2016, pp. 1-3.